Phosphoproteome dynamics reveal heat-shock protein complexes specific to the *Leishmania donovani* infectious stage

Miguel A. Morales[a], Reiko Watanabe[a], Mariko Dacher[a], Philippe Chafey[b,c], José Osorio y Fortéa[d,1], David A. Scott[e], Stephen M. Beverley[e], Gabi Ommen[f], Joachim Clos[f], Sonia Hem[g], Pascal Lenormand[g], Jean-Claude Rousselle[g], Abdelkader Namane[g], and Gerald F. Späth[a,2]

[a]Institut Pasteur, G5 Virulence Parasitaire, 75015 Paris, France; Institut National de la Santé et de la Recherche Médicale AVENIR and Centre National de la Recherche Scientifique (Unité de Recherche Associée 2581), 75015 Paris, France; [b]Institut Cochin, Université Paris Descartes, Centre National de la Recherche Scientifique (Unité Mixte de Recherche 8104), 75014 Paris, France; [c]Institut National de la Santé et de la Recherche Médicale, U1016, 75014 Paris, France; [d]Institut Pasteur, Unité d'Immunophysiologie et Parasitisme Intracellulaire, 75015 Paris, France; [e]Department of Molecular Microbiology, Washington University School of Medicine, St. Louis, MO 63110; [f]Leishmaniasis Research Group, Bernhard Nocht Institute for Tropical Medicine, D-20359 Hamburg, Germany; and [g]Institut Pasteur, Plate-forme de Protéomique and Centre National de la Recherche Scientifique Unité de Recherche Associée 2185, Department of Structural Biology and Chemistry, Pasteur-Genopole Ile-de-France, 75015 Paris, France

Edited by Elizabeth Anne Craig, University of Wisconsin, Madison, WI, and approved March 23, 2010 (received for review December 23, 2009)

Leishmania **is exposed to a sudden increase in environmental temperature during the infectious cycle that triggers stage differentiation and adapts the parasite phenotype to intracellular survival in the mammalian host. The absence of classical promoter-dependent mechanisms of gene regulation and constitutive expression of most of the heat-shock proteins (HSPs) in these human pathogens raise important unresolved questions as to regulation of the heat-shock response and stage-specific functions of *Leishmania* HSPs. Here we used a gel-based quantitative approach to assess the *Leishmania donovani* phosphoproteome and revealed that 38% of the proteins showed significant stage-specific differences, with a strong focus of amastigote-specific phosphoproteins on chaperone function. We identified STI1/HOP-containing chaperone complexes that interact with ribosomal client proteins in an amastigote-specific manner. Genetic analysis of STI1/HOP phosphorylation sites in conditional *sti1*$^{-/-}$ null mutant parasites revealed two phosphoserine residues essential for parasite viability. Phosphorylation of the major *Leishmania* chaperones at the pathogenic stage suggests that these proteins may be promising drug targets via inhibition of their respective protein kinases.**

signaling | stress response

Kinetoplastid parasites of the genus *Leishmania* generate a variety of pathologies collectively termed leishmaniasis, afflicting millions of people worldwide (1, 2). During the infectious cycle, these insect-borne parasitic trypanosomatids are exposed to a temperature increase following transmission from the invertebrate to the vertebrate host. The temperature change provides a crucial signal for developmental transition of the promastigote insect form to the amastigote form that thrives inside host phagocytes, generating the disease (3). Despite the relevance of heat-induced stage differentiation for pathogenesis, mechanisms underlying the parasite heat-shock response and its role in the development and survival of the amastigote stage remain poorly understood.

Trypanosomatids express highly conserved members of heat-shock and chaperone protein families, suggesting that the cellular response to heat stress is similar between parasite and host (4, 5). However, in contrast to other eukaryotes that regulate heat-induced expression of molecular chaperones and cytoprotective proteins via a family of heat-shock transcription factors (HSFs) (6), trypanosomatid genomes do not encode for classical transacting nuclear factors (7). Gene expression in these organisms relies on highly parasite-specific mechanisms involving polycistronic transcription and transsplicing (8, 9). Expression of the major heat-shock proteins (HSPs) is constitutive, even if heat shock may induce a transient increase in synthesis, which has been shown to be regulated exclusively at the posttranscriptional level (10–13). In contrast to its vertebrate host, both constitutive and inducible expression of *Leishmania* HSPs occurs from the same set of genes, making constitutive and stress-inducible chaperones indistinguishable at the sequence level (11, 14). This important difference in host and parasite biology raises questions concerning the role of *Leishmania* HSPs at low temperatures in promastigotes and regulation of their chaperone function upon temperature increase in differentiating and proliferating amastigotes. By combining approaches of quantitative phosphoproteomics, systems biology, and mutagenesis, we have uncovered several unique properties of *Leishmania donovani* HSPs with respect to protein modifications, complex formation, and the importance of chaperone phosphorylation in parasite viability.

Results and Discussion

Two-dimensional differential gel electrophoresis (2D-DIGE) analysis of affinity-enriched phosphoextracts obtained from *L. donovani* LD1S promastigotes and axenic amastigotes (15, 16) revealed dramatic differences in protein phosphorylation profiles across the major *Leishmania* infectious stages (Fig. 1*A*, Fig. S1*B*, and Dataset S1). A total of 831 protein spots were detected automatically using the DeCyder Differential Analysis Software Package (GE Healthcare), and >700 spots matched between three gels representing independent biological replicates, indicating little experimental variation between samples and highly reproducible two-dimensional gel electrophoresis (2DE) conditions (Dataset S1). A total of 171 proteins were identified by mass spectrometry using the genome database of highly related *Leishmania infantum* (WWW.GeneDB.org) (Fig. S1*A* and Dataset S1), including 55 putative phosphoproteins not identified in our previous study using fluorescent multiplex staining (17). Gene ontology (GO) analysis of the *Leishmania* phosphoprotein dataset via yeast ortholog mapping (Dataset S2) identified six statistically

Author contributions: M.A.M. and G.F.S. designed research; M.A.M., R.W., M.D., G.O., S.H., P.L., and J.-C.R. performed research; P.C., J.O.y.F., D.A.S., and S.M.B. contributed new reagents/analytic tools; M.A.M., J.C., A.N., and G.F.S. analyzed data; and G.F.S. wrote the paper.

The authors declare no conflict of interest.

This article is a PNAS Direct Submission.

Freely available online through the PNAS open access option.

[1]Present address: Limagrain Europe, Biometry Department, ZAC les portes de Riom, 63204 Riom, France.

[2]To whom correspondence should be addressed. E-mail: gerald.spaeth@pasteur.fr.

This article contains supporting information online at www.pnas.org/lookup/suppl/doi:10.1073/pnas.0914768107/-/DCSupplemental.

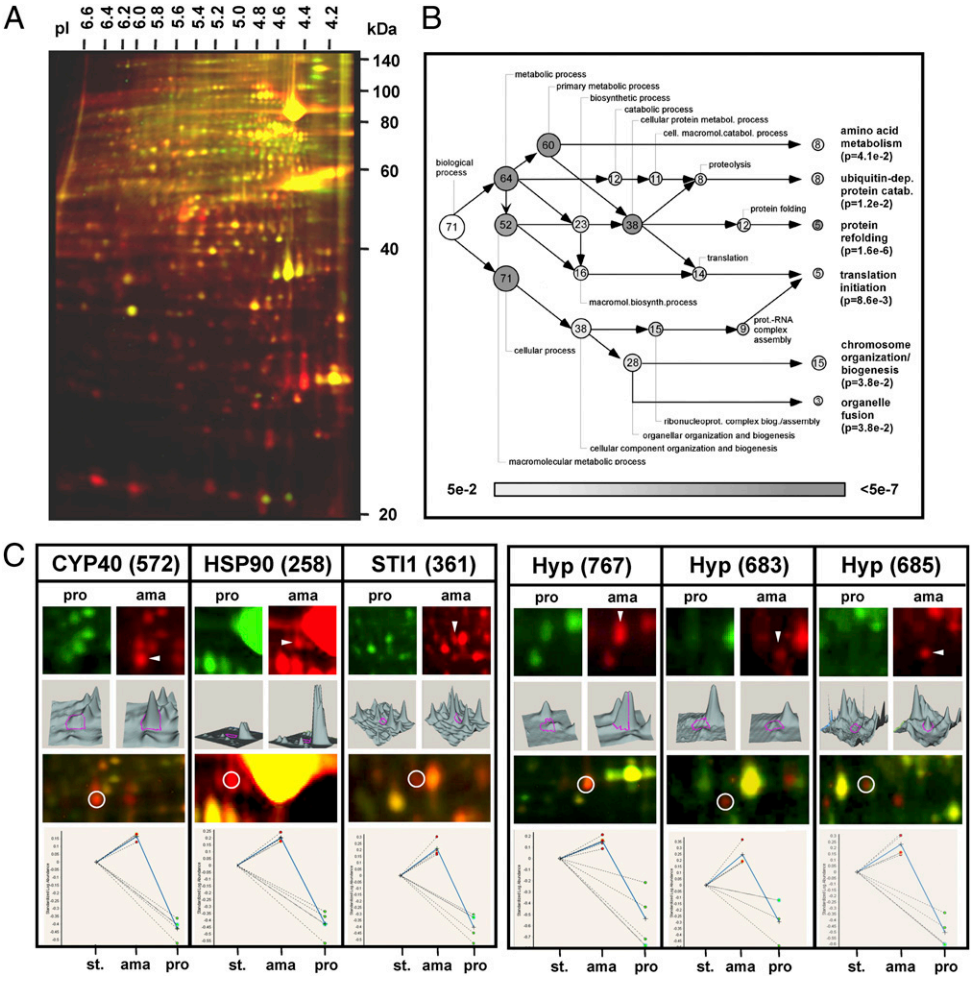

Fig. 1. Quantitative analysis of *L. donovani* stage-specific phosphoproteome. (*A*) 2D-DIGE analysis. Extracts from promastigotes and host-free amastigotes of three independent biological repeat experiments were differentially labeled with the spectrally resolvable CyDye fluors Cy3 and Cy5 and separated by two-dimensional electrophoresis (2DE) on 11-cm (pH 4–7) IPG strips and 12.5% polyacrylamide gels. A merged image of Cy5-labeled amastigotes (red) and Cy3-labeled promastigotes (green) is shown. The molecular weights of marker proteins (kDa) and the pH of the gradient (pI) are indicated. (*B*) Gene ontology analysis. Overrepresented categories of GO biological processes identified with the BiNGO plugin and visualized with Cytoscape software are shown. Gray levels indicate type I error level (hypergeometric test *P* value) after false discovery rate correction. Branches of the network selected for statistical significance are represented (*P* values <5e-02). The node area is proportional to the number of genes that correspond to a given GO category. (*C*) Analysis of the amastigote phosphoproteome. The readout of the DeCyder Biological Variation Analysis (BVA) module is shown for the most abundant amastigote phosphoprotein cyclophilin 40 (CYP40, spot 572); one isoform of HSP90 (spot 258); stress-induced protein STI1 (spot 361); and hypothetical proteins LinJ15.0040 (spot 767), LinJ32_V3.2410 (spot 683), and LinJ04.0240 (spot 685). Enlarged regions of 2D-DIGE gels for Cy3-labeled promastigotes (pro, green) and Cy5-labeled amastigotes (ama, red), and the corresponding 3D views, are represented. The *Bottom* shows a graphic representation of differences in abundance of these proteins across three independent experiments. For normalization purposes, a Cy2-labeled internal standard was included, corresponding to a pool of protein from all extracts used in the analysis (st, standard).

significant GO categories that were overrepresented in our analysis (Fig. 1*B* and Table S1). Three of these processes—translation initiation, protein folding, and protein catabolism—have been implicated previously in trypanosomatid differential gene expression (9), emphasizing the importance of protein phosphorylation in posttranslational control of this process.

We previously analyzed affinity-enriched *L. donovani* phosphoproteins by qualitative 2DE analysis and demonstrated the specificity of this procedure combining fluorescent phosphoprotein staining and phosphatase treatment (17). In contrast to this analysis, which suggested only little stage-specific phosphorylation, the quantitative 2D-DIGE analysis revealed a statistically significant difference (*P* value <0.05) in protein abundance for 318 spots corresponding to 38% of the detected phosphoproteins, with 10.2% of the phosphoproteins showing a statistically significant increase in abundance at the amastigote stage of ≥2-fold (Fig. S1*B* and Dataset S1). Significantly, amastigote phosphoproteins with increased abundance and thus phosphorylation compared to promastigotes were almost exclusively protein chaperones, including several isoforms of HSP90 family member HSP83 (hereafter referred to as HSP90), various HSP70 family members, stress-induced protein STI1/HOP (referred to hereafter as STI1) (18), cyclophilin 40, and the *L. donovani* ortholog of tetratricopeptide repeat (TPR) domain-containing peptidyl-prolyl-isomerase-like protein LinJ19_V3.1560 (Fig. 1*C* and Table S2). Previous proteomic studies that quantified changes in protein abundance during axenic amastigote differentiation (Fig. S2) (14), along with quantitative Western blot analysis of promastigote and amastigote total and phosphoextracts (Fig. 2*A*), demonstrate that the expression of these protein chaperones across the promastigote and amastigote stages is largely constitutive and not induced by elevated temperature. The increased abundance of these HSPs and chaperones in the amastigote phosphoproteome therefore does not simply result from increased expression, but rather reflects a change in phosphorylation stoichiometry with, for example, an 8-fold increase in the phosphorylation ratio of STI1 at the intracellular stage (Fig. 2*A*).

Evidence for a potential regulatory role of HSP phosphorylation in *Leishmania* arises from MALDI-TOF/TOF mass spectrometry analysis of the phosphorylation sites of HSP90 and HSP70. Phosphopeptides were isolated after in-gel digestion and peptide extraction from the 2D gels by TiO_2 enrichment (Fig. 2*B* and Fig. S3*A*). Manual analysis of the mass spectrometry spectra identified three phosphorylation sites at HSP90 Thr223 and Ser526 and at HSP70 Thr498. Conservation of the threonine residues between *Leishmania* and human HSP90 and HSP70 identifies this residue as a putative phosphorylation site in higher eukaryotes as well (Fig. 2*C* and Fig. S3*B*). Significantly, whereas the Thr223 residue in *L. donovani* HSP90 corresponds to serine in human HSP90 and thus may be regulated by phosphorylation, HSP90 Ser526 is unique to *Leishmania* despite the highly conserved sequence to the human homolog (Fig. 2*C*). The presence

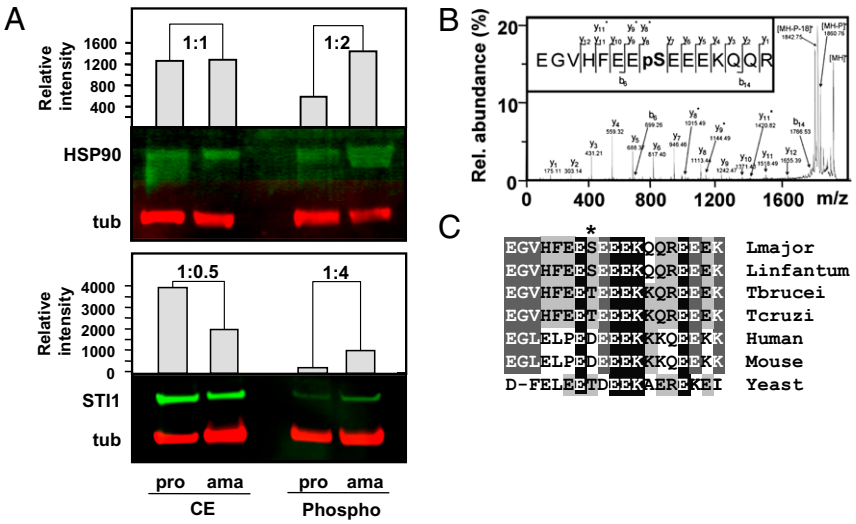

Fig. 2. Analysis of phosphoprotein stoichiometry and phosphorylation site determination. (*A*) Quantitative Western blot. Promastigote (pro) and amastigote (ama) crude (CE) and phosphoprotein (Phospho) extracts were analyzed by Western blotting using polyclonal anti-*Leishmania* HSP90 and STI1 and monoclonal anti-tubulin (tub) antibodies. The blots were revealed using ZyMax Cy3-conjugated anti-rabbit and ZyMax Cy5-conjugated anti-mouse secondary antibodies (Invitrogen) and signals were detected using a Typhoon variable mode imager. Relative intensities correspond to quantified signals of HSP90 and STI1 after normalization to α-tubulin (ImageQuant software; GE Healthcare). (*B*) Phosphopeptide analysis. MALDI-TOF/TOF spectrum of one HSP90 peptide isolated from 2D-DIGE gels after tryptic digestion and TiO_2 enrichment is shown. Peptide 519EGVHFEESEEEKQQR533 (*m/z* 1940.00) of HSP90 contains y_7, y_8, and y_8* ions, enabling identification of Ser526 as the phosphorylated residue. *, fragment ions arising from loss of phosphoric acid (−98 Da); $[MH]^+$, precursor ion; $[MH\text{-}P\text{-}18]^+$, precursor ion with loss of one phosphoric acid (−98 Da); pS, phosphorylated serine. (*C*) Multiple alignments. Sequence elements encompassing HSP90 phosphorylation sites of three trypanosomatids, human and yeast, were analyzed with ClustalXv2. The phosphoresidue is marked by the asterisk.

of this phosphorylation site opens up the possibility that the function of this major HSP is regulated in a parasite-specific manner by changes in the protein ionic state through phosphorylation, which may affect protein conformation and interaction with other chaperones, thus adding new regulatory features to *L. donovani* HSP90. Whereas this phosphorylation site is conserved in *Trypanosoma* HSP90 as judged by multiple alignment (Fig. 2*C*), this position is occupied in human and mouse HSP90 by aspartic acid. Thus, the HSP90 configuration in higher eukaryotes may be locked into a conformation that mimics constitutive phosphorylation. These findings indicate that regulation of HSP90 functions through posttranslational modifications may substantially differ between parasite and host despite the highly conserved sequence of this protein from *Leishmania* to man.

Biological network analysis using PathwayArchitect software applied to the identified parasite phosphoprotein datasets revealed the presence of a protein network formed between six amastigote phosphoproteins (Fig. 3*A*, Table S3). In other eukaryotes, this multimeric chaperone complex has been shown to provide an important signaling function through its interaction with so-called "client proteins," which include various steroid receptors and protein kinases (19, 20). Cochaperone STI1 plays a crucial role in formation of this complex, acting as a scaffolding protein that mediates the interaction between HSP90 and the HSP70/client protein complexes through specific TPR-rich domains (21, 22). We investigated the presence of the predicted STI1-containing protein complexes in *Leishmania* by Blue Native (BN) electrophoresis and Western blot analysis. Amastigote-specific phosphorylation of multiple protein chaperones correlated with the presence of numerous STI1-containing complexes ranging from 66 to 480 kDa (Fig. 3*B*). As judged by coimmunoprecipitation using anti-STI1 antibody, only the amastigote STI1/HSP90 complex interacts with HSP70/client protein complexes (Fig. 3*C*). Mass spectrometry analysis of the coprecipitated protein bands identified numerous client proteins implicated in the assembly of the protein translation machinery and the control of protein translation (Fig. 3*D*). The specificity of this interaction has been controlled for by using an isotype-specific control antibody (Fig. S3*C*) and is further supported by the absence of client protein detection in promastigotes, despite their constitutive expression at both stages (23). Our data correlate STI1 phosphorylation with complex formation linked to protein translation, which may affect resistance of ribosomal client proteins against proteasome-dependent degradation (24). Although we detected these complexes only in amastigotes, our data do not rule out the presence of similar complexes in promastigotes, which may have escaped our analysis due to their low abundance. These results are reminiscent of the observation that phosphorylation of murine STI1 affects localization of this protein and thus the types of client proteins that interact with STI1/HSP90/HSP70 (25).

We next used a genetic approach to investigate the biological significance of STI1 phosphorylation by mutagenesis. Three *STI1* phospho-site mutants were generated on the basis of previously identified STI1 phosphoresidues in *Trypanosoma brucei* (26), mouse (27), and human (28) (Fig. 4*A*). As *STI1* appears to be essential, we tested these mutants using a conditional knockout system (29). In this approach, to guard against the lethal phenotype, both chromosomal *STI1* alleles were inactivated in the presence of an episomal plasmid expressing WT *STI1*, yielding the mutant *sti1*$^{-/-}$/pXNG-*STI1* (Fig. 4*B* and Fig. S4). The episomal plasmid pXNG4SAT (29) additionally carries both a fluorescent (GFP) and a negative selectable thymidine kinase (TK) marker rendering parasites susceptible to the antiviral drug ganciclovir (GCV). Thus by FACS or drug selection *sti1*$^{-/-}$/pXNG-*STI1* parasites could be tested for their requirement to maintain the ectopic *STI1* gene copy. The functionality of mutated *STI1* genes was then tested in a "plasmid shuffle" (30), by introducing a second plasmid, and asking whether the WT *STI1* borne on pXNG could be lost. As expected for an essential gene, it was not possible to segregate away pXNG-*STI1* in the chromosomal *sti1*$^{-/-}$ null mutant, even in the presence of GCV (Fig. 4*C*, parental line). The presence of an additional copy of functional *STI1*, however, allowed for efficient elimination of pXNG-*STI1* during negative selection as judged by the substantial reduction in GFP fluorescence intensity (STI1_WT, Fig. 4 *C* and *D Left*).

This binary readout allowed us now to test for the functionality of the *STI1* phosphorylation site mutants. The mutants were expressed in independent *sti1*$^{-/-}$/pXNG-*STI1* clones, and their effect on negative selection against pXNG-*STI1* was analyzed. Expression of the T217A mutant fully compensated for pXNG-*STI1*, which was efficiently eliminated during negative selection (Fig. 4 *C* and *D*). This result suggests that the T217A mutation does not affect the functional properties of STI1 (case 2, Fig. 4*B*). In contrast, expression of neither S15A nor S481A was able to compensate for pXNG-*STI1*, which was maintained at levels comparable to the *sti1*$^{-/-}$/pXNG-*STI1* parental line in both

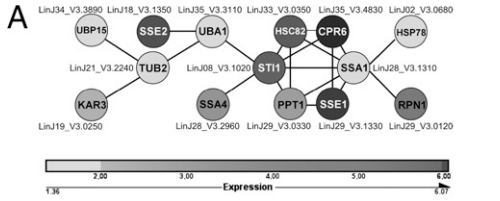

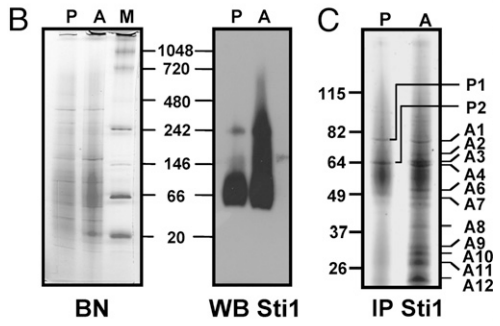

D

ID	Name	Acc.no	MW	peptides
P1	HSP83-1	LinJ33_V3.0350	79388,8	14
P2	STI1	LinJ08_V3.1020	62770,3	13
A1	HSP83-1	LinJ33_V3.0350	79388,8	19
A2	HSP70	LinJ28_V3.2960	71509	14
A3	RNA helicase	LinJ32_V3.0410	67223,2	11
A4	STI1	LinJ08_V3.1020	62770,3	9
A5	n.d.			
A6	6p1-fructokinase	LinJ29_V3.2620	54584,2	9
A7	rib. protein l3	LinJ32_V3.3330	47820,9	12
A8	rib. protein L1a	LinJ29_V3.1170	48243,8	11
A9	40S rib. prot. S3a	LinJ35_V3.0400	30247,1	6
A10	60S rib. prot. L13	LinJ29_V3.2580	24902,3	10
A11	40S rib. prot. S6	LinJ21_V3.2150	28315,8	14
	60S rib. prot. L2	LinJ35_V3.1440	28597,1	6
A12	40S rib. prot. S8	LinJ24_V3.2160	25003,9	5
	60S rib. prot. L13a	LinJ34_V3.0910	25572,1	8
	60S rib. protein L7	LinJ26_V3.0150	31179,6	10
	40S rib. protein SA	LinJ36_V3.5350	27795,1	8

Fig. 3. Chaperone phosphorylation in amastigotes is linked to formation of a stage-specific multiprotein complex. (*A*) Biological network analysis. Analysis was carried out with PathwayArchitect software (version 3.0.1; www.stratagene.com). An input set of 43 yeast IDs was used to build the biological interaction network from annotations extracted from scientific literature (automatic scanning of abstracts from PubMed database: www.ncbi.nlm.nih.gov/pubmed). Shaded levels indicate the fold increase in amastigote phosphoprotein abundance compared to promastigote phosphoextracts. (*B*) Blue-Native PAGE. Native extracts from promastigotes (P) or amastigotes (A) were separated on NativePAGE Novex 4–16% Bis-Tris gels (Invitrogen) and complexes were revealed by colloidal Coomassie staining (*Left*). Replica gels were electroblotted onto PVDF membranes and proteins detected with anti-STI1 antibody (*Right*). Molecular weight (MW) of native protein marker (M) is shown. (*C*) Coimmunoprecipitation. Pro- (P) and amastigote (A) crude extracts were incubated with STI1 polyclonal antibody and protein A MicroBeads (Miltenyi Biotec). Eluates were separated by denaturing SDS/PAGE and stained with SyproRuby. MW of marker proteins in kDa is shown. (*D*) STI1-associated proteins isolated by immunoprecipitation were identified by MS/MS analysis.

promastigote and amastigote stages (Fig. 4 *C* and *D*). Together these data suggest that the STI1 residues S15 and S481 are essential phosphorylation sites (case 1, Fig. 4*B*) required for *L. donovani* viability in culture and emphasize the importance of chaperone phosphorylation in parasite biology. Further analysis of the role of these phosphorylation sites in STI1 complex formation was precluded by the lethal *sti1*$^{-/-}$ phenotype and the requirement to maintain WT STI1.

The manner in which *Leishmania* regulates the response to stress is fundamentally different from that of other eukaryotes, including the mammalian host. In most organisms, stress-induced expression increases stress tolerance through protection of basic cell functions, without a major impact on cellular morphology and phenotype. In *Leishmania*, however, stress signals such as low pH and nutritional starvation, or high temperature, induce developmental programs that lead to differentiation of metacyclic promastigotes and amastigotes and adapt the parasite for transmission and intracellular survival (3, 31, 32). This reinterpretation of the stress response likely translates into unique regulatory mechanisms and interactions of *Leishmania* chaperones. Our data provide important insights into these parasite-specific mechanisms, which may depend on (*i*) stage-specific chaperone phosphorylation during environmentally induced parasite differentiation; (*ii*) phosphorylation of unique residues in parasites HSP70, HSP90, and STI1; and (*iii*) formation of chaperone complexes. The emphasis on posttranslational regulation of the stress response in *Leishmania* through phosphorylation and other protein modifications may represent an evolutionary adaptation of trypanosomatid parasites to constitutive expression and the absence of transcriptional regulation (9). By analogy to stress regulation through HSFs in other eukaryotes (33), our data indicate that the absence of these factors in trypanosomatids may have been compensated for by the evolution of protein kinases that regulate chaperone function. In resting cells, HSF1 is inactivated in other eukaryotes through its association with HSP70 and HSP90, but is released and activated under stress conditions (34). In a similar fashion, *Leishmania* chaperones may tether protein kinases that are released and activated during environmentally induced stage differentiation. Indeed, binding of *Leishmania* MAP kinases to HSP70 (35) and the direct implication of HSP90 in parasite differentiation established in geldanamycin-treated parasites (36) suggest a unique model in which chaperone/kinase interactions would regulate phosphotransferase activities, which in turn might directly feed back on chaperone functions and differentiation.

Materials and Methods

Cell Culture and Differentiation of *L. donovani*. The *L. donovani* strain 1S2D (MHOM/SD/62/1S-CL2D), clone LdB was cultured and axenic amastigotes were differentiated as described (16, 37).

Preparation of *L. donovani* total and phosphoprotein extracts. Axenic promastigotes or axenic amastigotes 48 h after induction of differentiation by pH and temperature shift were harvested from logarithmic cultures. For phosphoprotein purification, protein concentration was adjusted to 0.1 mg/mL, and 2.5-mg extracts were applied onto equilibrated affinity columns of the phosphoprotein purification kit (Qiagen) according to manufacturer's instructions.

Western Blot Analysis. Proteins were revealed using the following antibodies: polyclonal anti-STI-1 (18) and anti-HSP83, mouse monoclonal anti-α-tubulin antibody (Sigma), and anti-rabbit or anti-mouse ZyMax Cy3 or Cy5 conjugated secondary antibodies (Invitrogen). In some experiments, NativePAGE Novex 4–16% Bis-Tris Gels (Invitrogen) were transferred onto PVDF membranes, and proteins were revealed using the antibodies described above and anti-rabbit HRP-conjugated secondary antibodies (Pierce).

Immunoprecipitation. Cells were lysed and incubated for 45 min at 4 °C with STI-1 polyclonal antibody (10 μL, 200 μg/mL) and protein A MicroBeads (50 μL; Miltenyi Biotec). Mixtures were loaded on μMACS columns (Miltenyi Biotec). Eluates were separated by denaturing SDS/PAGE, gels were stained with SyproRuby, and bands of interest were excised and further analyzed by MS-MS/MS.

Blue Native PAGE. Native extracts were centrifuged at 20,000 × *g* for 30 min at 4 °C. Twenty or 40 μg of protein, containing 0.025% Coomassie Blue G-250, were separated on NativePAGE Novex 4–16% Bis-Tris Gels (Invitrogen) at 150 V for 3 h and 250 V for 1 h at 4 °C.

Sample Preparation and DIGE Labeling. Phosphoprotein pellets were resuspended in DIGE sample buffer (7 M Urea, 2 M Thiourea, 4% CHAPS, 30 mM Tris, pH 8.5) to a final protein concentration of 5.0 mg/mL. Phosphoprotein extracts from promastigotes and amastigotes were differentially labeled with the spectrally resolvable Cy3 and Cy5, and a pool of both extracts was labeled with Cy2 for normalization purposes, following the manufacturer's recommendations (GE Healthcare). Three independent biological replicates of promastigote and amastigote phosphoextracts were prepared and resolved by 2D-DIGE. In addi-

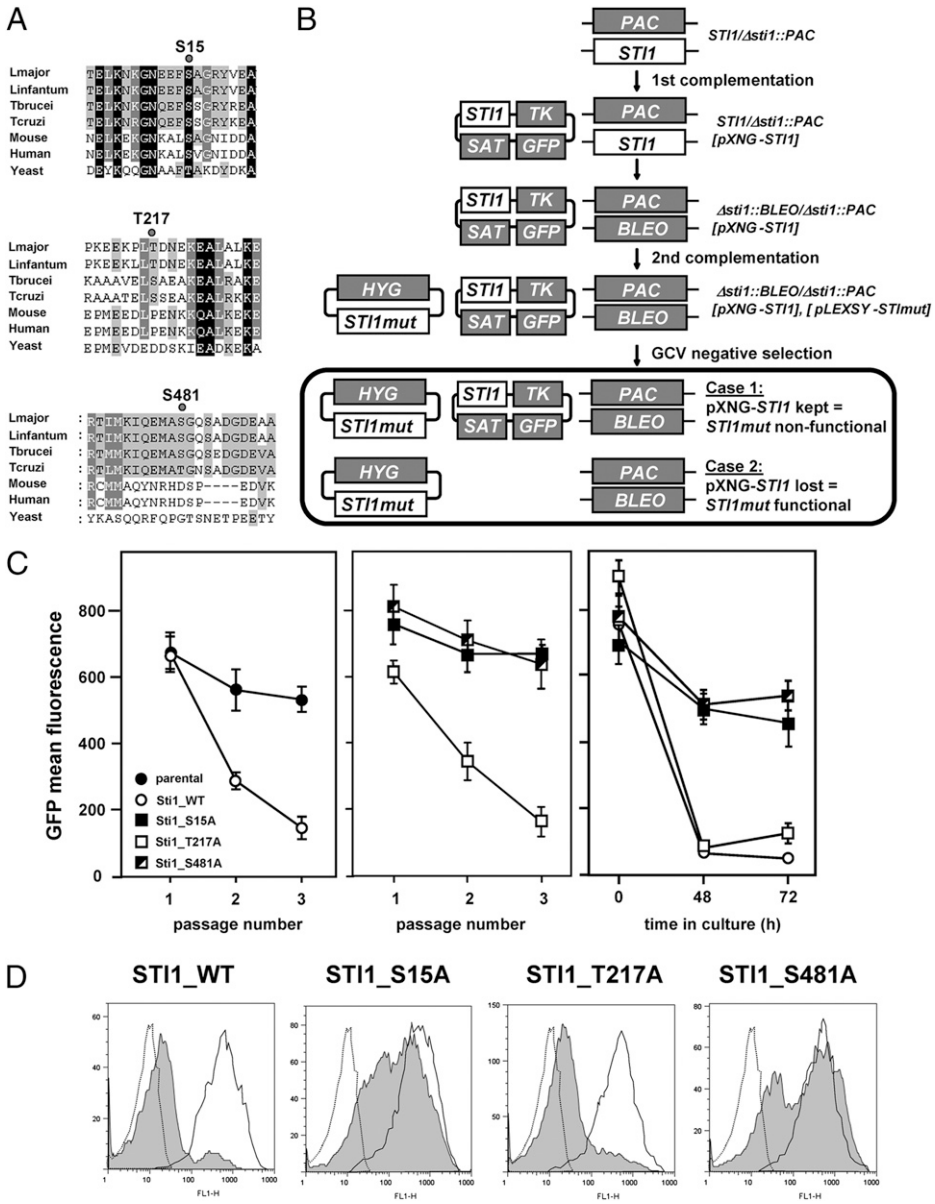

Fig. 4. STI1 phosphorylation is essential for *L. donovani* viability. (*A*) Multiple alignment of STI1 homologs from *Leishmania major* (Lmajor, CAJ02290.1), *L. infantum* (Linfantum, CAM65800.1), *Trypanosoma brucei* (Tbrucei, CBH11274.1), *Trypanosoma cruzi* (Tcruzi, EAN97552.1), *Mus musculus* (Mouse, AAC53267.1), *Homo sapiens* (Human, AAA58682.1), and *Saccharomyces cerevisiae* (Yeast, CAA60743.1) using ClustalXv2 is shown. The number indicates the *L. major* STI1 amino acids targeted for analysis by mutagenesis using the QuikChange Site-Directed Mutagenesis Kit (Stratagene). Phosphorylation sites at serine 15 (S15) and serine 481 (S481) have been experimentally identified in human and *T. brucei*, respectively (26, 28). Threonine 217 (T217) has been selected on the basis of experimentally identified threonine phosphorylation upstream of the yeast STI1 nuclear localization signal (NLS, dotted line) and the presence of a casein kinase II signature sequence S/T-X-X-D/E (27). The shading indicates the level of amino acid conservation. (*B*) Generation of *L. donovani sti1*$^{-/-}$ conditional null mutants for analysis of phosphorylation site-specific mutants. Heterozygous *sti1*$^{+/-}$ null mutants (*STI1/Δsti1::PAC*) were transfected with episomal vector pXNG carrying the *STI1* wild-type ORF (*STI1/Δsti1::PAC[pXNG-STI1]*), before replacement of the second *STI1* allele yielding homozygous *sti1*$^{-/-}$ null mutants (*Δsti1::BLEO/Δsti1::PAC[pXNG-STI1]*). Independent clones were transfected with episomal vector pLEXSY expressing either an additional copy of wild-type *STI1* or one of the phospho-site mutants described in *A*. The ability of episomally expressed *STI1* phospho-site mutants S15A, T217A, and S481A to complement for the loss of pXNG-*STI1* during negative selection with gangciclovir (GCV) provides a genetic test to distinguish mutations that affect STI1 function (case 1, pXNG-*STI1* is maintained) from silent mutations (case 2, pXNG-*STI1* is lost). Selections were performed using 25 μg/mL puromycin, 150 μg/mL nourseothricin, 5 μg/mL bleomycin, and 50 μg/mL hygromycin B, respectively. *BLEO*, bleomycin resistance cassette; GCV, ganciclovir; *GFP*, green fluorescent protein gene; *HYG*, hygromycin B resistance cassette; *PAC*, puromycin resistance cassette; *SAT*, nourseothricin resistance cassette; *TK*, herpes simplex virus thymidine kinase gene. (*C*) Analysis of *STI1* mutants by negative selection in conditional *sti1*$^{-/-}$ lines. Elimination of pXNG-*STI1* was followed by FACS analysis monitoring the levels of GFP expressed from the same episome. GFP mean fluorescence of conditional *sti1*$^{-/-}$ null mutant promastigotes treated for three culture passages with 50 μg/mL GCV (*Left* and *Center*) or axenic amastigotes treated for 72 h with GCV (*Right*) is shown. Data are means ± SD of a representative experiment analyzed in triplicate. (*D*) Histogram plots of one representative analysis of axenic amastigotes after 72 h of GCV selection (shaded histograms). Dotted lines represent the background fluorescence of untransfected control parasites. Solid lines represent the GFP fluorescence levels of parasites cultured without GCV.

tion, a gel containing a pool of either pro- or amastigote extracts from all extractions was included for normalization purposes.

2DE. A total of 90 μg of protein sample containing 30 μg of Cy3- and Cy5-labeled samples was pooled together with 30 μg of Cy2-labeled control and adjusted with 150 μL Destreak rehydration buffer (GE Healthcare) containing 0.5% IPG buffer 4-7 and 1.0% DTT. Samples were simultaneously separated in the first dimension by iso-electric focusing (IEF) overnight (see *SI Materials and Methods* for details).

Staining Procedures and Image Analysis. After electrophoresis, gels were scanned on a Typhoon 9410 Variable Mode Imager (GE Healthcare) and analyzed with DeCyder 6.5 software (GE Healthcare).

Protein Identification by Mass Spectrometry. Spots of interest were excised from gels using the ProPic Investigator robotic system (Genomic Solutions). MS and MS/MS raw data for protein identification were obtained as previously described (17) (see *SI Materials and Methods* for details).

Phosphopeptide Identification. Protein digests, obtained as described above, were diluted in loading buffer (80% ACN, 5% TFA) (38) and loaded on TiO_2 microcolumns as described previously (39). All phosphorylated peptides were first analyzed for the presence of the major fragment ion $[MH\text{-}H_3PO_4]^+ = MH - 98$ Da corresponding to the loss of the phosphate moiety and identified positively by MASCOT. In addition, all MS/MS spectra were carefully curated manually for assignment of phosphorylation sites (see *SI Materials and Methods* for details).

Bioinformatics Approaches. Retrieval of yeast orthologous sequences was carried out with a BLASTP algorithm (40) by querying the *Saccharomyces cerevisiae* protein database with the *L. infantum* protein sequences (default parameters; Refseq protein database build 2.1 released May 17, 2005; www.ncbi.nlm.nih.gov/genome/seq/BlastGen/BlastGen.cgi?taxid=4932). From 92 unique *L. infantum* IDs used in this analysis, 17 IDs were specific to *Leishmania* and 75 IDs mapped to 71 yeast orthologs with expectation values ranging from $E = 0$ to $E = 0.003$ and alignment scores ranging from 974 to 38.9 bits. Functional enrichment analysis was carried out with the 71 yeast IDs as input using the BiNGO plugin (version 2.1) of the Cytoscape software (version 2.5.1). Biological network analysis was carried out with PathwayArchitect software (version 3.0.1; www.stratagene.com). An input set of 43 yeast IDs was used to build the biological interaction network from the annotations extracted from the scientific literature (automatic scanning of abstracts from PubMed database; www.ncbi.nlm.nih.gov/pubmed/).

ACKNOWLEDGMENTS. We thank Dr. Zilberstein (Technion, Israel) for anti-HSP83 antiserum, Dr. Reed (Infectious Disease Research Institute, Seattle) for anti-STI1 antibody, and Malcolm McConville for critical reading of the manuscript. This work was supported by the Institut National de la Santé et de la Recherche Médicale AVENIR program (G.F.S., M.A.M., R.W.), National Institutes of Health Grants AI-21903 and AI-29646 (to S.M.B.), the 7th Framework Programme of the European Commission through a grant to the LEISHDRUG Project (223414), and the Fondation de Recherche Medicale Equipe Fondation pour la Recherche Médicale program (DEQ20061107966).

1. Ashford R, Desjeux P, Raadt P (1992) Estimation of population at risk of infection and number of cases of Leishmaniasis. *Parasitol Today* 8:104–105.
2. Bañuls AL, Hide M, Prugnolle F (2007) Leishmania and the leishmaniases: A parasite genetic update and advances in taxonomy, epidemiology and pathogenicity in humans. *Adv Parasitol* 64:1–109.
3. Zilberstein D, Shapira M (1994) The role of pH and temperature in the development of Leishmania parasites. *Annu Rev Microbiol* 48:449–470.
4. Clos J (1997) *Heat Shock Proteins in Biology and Disease*, eds Radons J, Multhoff G (Research Signpost, Kerala, India), pp 421–448.
5. Folgueira C, Requena JM (2007) A postgenomic view of the heat shock proteins in kinetoplastids. *FEMS Microbiol Rev* 31:359–377.
6. Morimoto RI (1998) Regulation of the heat shock transcriptional response: Cross talk between a family of heat shock factors, molecular chaperones, and negative regulators. *Genes Dev* 12:3788–3796.
7. Ivens AC, et al. (2005) The genome of the kinetoplastid parasite, *Leishmania major*. *Science* 309:436–442.
8. Clayton C, Shapira M (2007) Post-transcriptional regulation of gene expression in trypanosomes and leishmanias. *Mol Biochem Parasitol* 156:93–101.
9. Clayton CE (2002) Life without transcriptional control? From fly to man and back again. *EMBO J* 21:1881–1888.
10. Argaman M, Aly R, Shapira M (1994) Expression of heat shock protein 83 in Leishmania is regulated post-transcriptionally. *Mol Biochem Parasitol* 64:95–110.
11. Brandau S, Dresel A, Clos J (1995) High constitutive levels of heat-shock proteins in human-pathogenic parasites of the genus Leishmania. *Biochem J* 310:225–232.
12. de Carvalho EF, de Castro FT, Rondinelli E, Soares CM, Carvalho JF (1990) HSP 70 gene expression in *Trypanosoma cruzi* is regulated at different levels. *J Cell Physiol* 143: 439–444.
13. Hunter KW, Cook CL, Hayunga EG (1984) Leishmanial differentiation in vitro: Induction of heat shock proteins. *Biochem Biophys Res Commun* 125:755–760.
14. Rosenzweig D, et al. (2008) Retooling Leishmania metabolism: From sand fly gut to human macrophage. *FASEB J* 22:590–602.
15. Barak E, et al. (2005) Differentiation of Leishmania donovani in host-free system: Analysis of signal perception and response. *Mol Biochem Parasitol* 141:99–108.
16. Goyard S, et al. (2003) An in vitro system for developmental and genetic studies of *Leishmania donovani* phosphoglycans. *Mol Biochem Parasitol* 130:31–42.
17. Morales MA, et al. (2008) Phosphoproteomic analysis of *Leishmania donovani* pro- and amastigote stages. *Proteomics* 8:350–363.
18. Webb JR, Campos-Neto A, Skeiky YA, Reed SG (1997) Molecular characterization of the heat-inducible LmSTI1 protein of *Leishmania major*. *Mol Biochem Parasitol* 89: 179–193.
19. Pratt WB, Galigniana MD, Harrell JM, DeFranco DB (2004) Role of hsp90 and the hsp90-binding immunophilins in signalling protein movement. *Cell Signal* 16:857–872.
20. Pratt WB, Morishima Y, Osawa Y (2008) The Hsp90 chaperone machinery regulates signaling by modulating ligand binding clefts. *J Biol Chem* 283:22885–22889.
21. Dittmar KD, Banach M, Galigniana MD, Pratt WB (1998) The role of DnaJ-like proteins in glucocorticoid receptor.hsp90 heterocomplex assembly by the reconstituted hsp90. p60.hsp70 foldosome complex. *J Biol Chem* 273:7358–7366.
22. Scheufler C, et al. (2000) Structure of TPR domain-peptide complexes: Critical elements in the assembly of the Hsp70-Hsp90 multichaperone machine. *Cell* 101:199–210.
23. Rosenzweig D, Smith D, Myler PJ, Olafson RW, Zilberstein D (2008) Post-translational modification of cellular proteins during *Leishmania donovani* differentiation. *Proteomics* 8:1843–1850.
24. Kim TS, et al. (2006) Interaction of Hsp90 with ribosomal proteins protects from ubiquitination and proteasome-dependent degradation. *Mol Biol Cell* 17:824–833.
25. Longshaw VM, Chapple JP, Balda MS, Cheetham ME, Blatch GL (2004) Nuclear translocation of the Hsp70/Hsp90 organizing protein mSTI1 is regulated by cell cycle kinases. *J Cell Sci* 117:701–710.
26. Nett IR, et al. (2009) The phosphoproteome of bloodstream form *Trypanosoma brucei*, causative agent of African sleeping sickness. *Mol Cell Proteomics* 8:1527–1538.
27. Blatch GL, Lässle M, Zetter BR, Kundra V (1997) Isolation of a mouse cDNA encoding mSTI1, a stress-inducible protein containing the TPR motif. *Gene* 194:277–282.
28. Dephoure N, et al. (2008) A quantitative atlas of mitotic phosphorylation. *Proc Natl Acad Sci USA* 105:10762–10767.
29. Murta SM, Vickers TJ, Scott DA, Beverley SM (2009) Methylene tetrahydrofolate dehydrogenase/cyclohydrolase and the synthesis of 10-CHO-THF are essential in *Leishmania major*. *Mol Microbiol* 71:1386–1401.
30. Sikorski RS, Boeke JD (1991) In vitro mutagenesis and plasmid shuffling: From cloned gene to mutant yeast. *Methods Enzymol* 194:302–318.
31. Sacks DL, Perkins PV (1984) Identification of an infective stage of Leishmania promastigotes. *Science* 223:1417–1419.
32. Zakai HA, Chance ML, Bates PA (1998) In vitro stimulation of metacyclogenesis in *Leishmania braziliensis, L. donovani, L. major* and *L. mexicana*. *Parasitology* 116: 305–309.
33. Kanei-Ishii C, Tanikawa J, Nakai A, Morimoto RI, Ishii S (1997) Activation of heat shock transcription factor 3 by c-Myb in the absence of cellular stress. *Science* 277:246–248.
34. Ali A, Bharadwaj S, O'Carroll R, Ovsenek N (1998) HSP90 interacts with and regulates the activity of heat shock factor 1 in *Xenopus* oocytes. *Mol Cell Biol* 18:4949–4960.
35. Morales MA, Renaud O, Faigle W, Shorte SL, Späth GF (2007) Over-expression of Leishmania major MAP kinases reveals stage-specific induction of phosphotransferase activity. *Int J Parasitol* 37:1187–1199.
36. Wiesgigl M, Clos J (2001) Heat shock protein 90 homeostasis controls stage differentiation in Leishmania donovani. *Mol Biol Cell* 12:3307–3316.
37. Saar Y, et al. (1998) Characterization of developmentally-regulated activities in axenic amastigotes of Leishmania donovani. *Mol Biochem Parasitol* 95:9–20.
38. Imanishi SY, et al. (2007) Reference-facilitated phosphoproteomics: Fast and reliable phosphopeptide validation by microLC-ESI-Q-TOF MS/MS. *Mol Cell Proteomics* 6: 1380–1391.
39. Hem S, Rofidal V, Sommerer N, Rossignol M (2007) Novel subsets of the Arabidopsis plasmalemma phosphoproteome identify phosphorylation sites in secondary active transporters. *Biochem Biophys Res Commun* 363:375–380.
40. Altschul SF, et al. (1997) Gapped BLAST and PSI-BLAST: A new generation of protein database search programs. *Nucleic Acids Res* 25:3389–3402.